http://ansinet.com/itj

ITJ

ISSN 1812-5638

INFORMATION TECHNOLOGY JOURNAL

ANSInet
Asian Network for Scientific Information
308 Lasani Town, Sargodha Road, Faisalabad - Pakistan

Information Technology Journal 13 (17): 2658-2665, 2014
ISSN 1812-5638 / DOI: 10.3923/itj.2014.2658.2665

Extended Range of Fin Stabilized Projectile Using Movable Canards

A. Elsaadany and YI Wen-Jun
National Key Laboratory, Nanjing University of Science and Technology,
200 XiaoLing Wie, XuanWu, Nanjing, Jiangsu, 210094, China

Abstract: The purpose of this study is to investigate the range extension capability for fin stabilized projectile using movable canard lifting surfaces. Performance evaluation of the advanced projectile in atmospheric flight is demonstrated using a six degree of freedom simulation model. Through comparison studies, the maximum range is shown to be extended by nearly double by commanding a full authority pitch maneuver at the trajectory's maximum altitude. A parametric analysis varying launch angle, canard deflection angle and canard lifting surface area are presented. Another analysis has been carried out for canards deployment times that verified the maximum extended range using simulation. In addition, the influence of the canards deflection rate on the projectile aerodynamic angle is demonstrated.

Key words: Trajectory prediction, fin stabilized projectiles, movable canards, range extension

INTRODUCTION

In the army field, there is always a need to achieve extended range for artillery projectiles without affecting their effectiveness. Typically, increases in maximum artillery range capability have been accomplished by increasing muzzle velocity of the projectile through the use of larger cannon and cannon propelling charges. The use of larger cannon with larger cannon propelling charges to achieve significantly extended range capability is limited by physical constraints of weight and size which adversely affect the mobility of the weapon. Another trend is improvement in projectile design which has similarly provided the means for increasing artillery maximum range capability. However, this improvement, individually, has inherent limitation. It is possible to simply incorporate a larger rocket motor at the expense of reduced payload/cargo in the projectile design configuration to achieve the desired maximum range goal. However, this would result in degradation in lethality, hence effectiveness. Some other concepts and modifications are proposed to extend the range of artillery projectile like course correction fuze. The Course Correction Fuze (CCF) concepts could provide an attractive and cost-effective solution for range extension. However, few studies have specifically addressed the use of canards to extend the range of a ballistic projectile. Typically, relatively small movable canards mounted on the front of the artillery projectile provide sufficient control authority to enable extended range and an accurate flight trajectory, as investigated by Rogers and Costello (2010) and Ollerenshaw and Costello (2008). Costello (1995, 1997) studied and evaluated the potential of range extension and accuracy improvement of a field artillery projectile using movable canard control.

In this study, a six degree-of-freedom (6-DOF) nonlinear model, in the atmospheric flight, is derived to predict the dynamic behavior of a fin stabilized projectile equipped with a movable canards. The model is developed based on Newton's equations of motion, taking into consideration the influence of the Earth's rotation and ellipsoidal shape. Furthermore, a modified standard atmospheric model to simulate air density and the speed of sound is used. This is followed by an investigation on the range extension capability for fin stabilized projectile using movable canard lifting surfaces. Results clarify that the maximum range can be extended by nearly double by commanding a full authority pitch maneuver at the trajectory's maximum altitude. With a representative canard configuration data, a parametric comparison analysis is achieved which includes different canard geometries and deflection angles. Analysis has been carried out for canards deployment times that verified the maximum range extension using simulation. In addition, the influence of the canards deflection rate on the projectile aerodynamic angle is demonstrated.

MATERIALS AND METHODS

Dynamic model: This section presents the equation of motion that model the projectile's atmospheric trajectory according to a set of initial launch conditions. As well as

Corresponding Author: A. Elsaadany, National Key Laboratory, Nanjing University of Science and Technology,
200 XiaoLing Wie, XuanWu, Nanjing, Jiangsu, 210094, China

the methodology used to compute forces and moments acting on the projectile body (Etkin, 2005; McCoy, 2012). The projectile is assumed to be both rigid (non-flexible) and rotationally symmetric about its spin axis. The translation dynamics give the projectile linear velocity as a result of the externally applied forces, whereas the rotation dynamics give its angular velocity as a function of the corresponding moments. The translational dynamic equations are obtained using a force balance equation on the projectile written in the body-fixed frame, given by:

$$\begin{Bmatrix}\dot{u}\\ \dot{v}\\ \dot{w}\end{Bmatrix}=\begin{Bmatrix}a_x^b\\ a_y^b\\ a_z^b\end{Bmatrix}=\frac{1}{m}\begin{Bmatrix}F_X\\ F_Y\\ F_Z\end{Bmatrix}-\begin{bmatrix}0 & -r & q\\ r & 0 & -p\\ -q & p & 0\end{bmatrix}\begin{Bmatrix}u\\ v\\ w\end{Bmatrix} \quad (1)$$

where, the terms F_X, F_Y and F_Z are the sum of weight, Magnus and aerodynamic forces resolved in the body-fixed reference frame. The rotational dynamic equations are obtained using a moment equation about the projectile mass center and written in the body-fixed frame, given by:

$$\begin{Bmatrix}\dot{p}\\ \dot{q}\\ \dot{r}\end{Bmatrix}=[I]^{-1}\left[\begin{Bmatrix}L\\ M\\ N\end{Bmatrix}-\begin{bmatrix}0 & -r & q\\ r & 0 & -p\\ -q & p & 0\end{bmatrix}[I]\begin{Bmatrix}p\\ q\\ r\end{Bmatrix}\right] \quad (2)$$

where, the terms L, M and N are the sum of steady aerodynamic, unsteady aerodynamic and magnus moments resolved in the body-fixed reference frame.

The rotational kinematic equations relate derivatives of Euler angles to angular velocity states are given by:

$$\begin{Bmatrix}\dot{\varphi}\\ \dot{\theta}\\ \dot{\psi}\end{Bmatrix}=\begin{bmatrix}1 & \sin\varphi\tan\theta & \cos\varphi\tan\theta\\ 0 & \cos\varphi & -\sin\varphi\\ 0 & \sin\varphi\sec\theta & \cos\varphi\sec\theta\end{bmatrix}\begin{Bmatrix}p_t\\ q_t\\ r_t\end{Bmatrix} \quad (3)$$

where, p_t, q_t and r_t are the angular acceleration components taking in account the error resulting from the Earth's rotation that expressed in terms of the vehicle-carried North East Down (NED) velocity and given by:

$$\begin{Bmatrix}p_t\\ q_t\\ r_t\end{Bmatrix}=\begin{Bmatrix}p\\ q\\ r\end{Bmatrix}-J_{BE}\begin{bmatrix}\left(\omega^e+\dot{\mu}\right)\cos\lambda\\ -\dot{\lambda}\\ -\left(\omega^e+\dot{\mu}\right)\sin\lambda\end{bmatrix} \quad (4)$$

$$J_{BE}=\begin{bmatrix}c\theta c\psi & s\varphi s\theta c\psi-c\varphi s\psi & c\varphi s\theta c\psi+s\varphi s\psi\\ c\theta s\psi & s\varphi s\theta s\psi+c\varphi c\psi & c\varphi s\theta s\psi-s\varphi c\psi\\ -s\theta & s\varphi c\theta & c\varphi c\theta\end{bmatrix} \quad (5)$$

where, sin and cos are abbreviated with s and c, respectively. The derivative of the geodetic position can be expressed in terms of the vehicle-carried NED velocity and given by:

$$\dot{\lambda}=V_N/\left(R_{mer}+h\right) \quad (6)$$

$$\dot{\mu}=V_E/\left(R_{norm}+h\right)\cos\lambda \quad (7)$$

$$\dot{h}=-V_D \quad (8)$$

The derivatives of the vehicle-carried NED velocity components taking in account Earth's rotation are, respectively given by:

$$\dot{V}_N=-\left(\dot{\mu}+2\omega^e\right)\sin\lambda\,V_E+\dot{\lambda}\,V_D+a_N \quad (9)$$

$$\dot{V}_E=\left(\dot{\mu}+2\omega^e\right)\sin\lambda\,V_N+\left(\dot{\mu}+2\omega^e\right)\cos\lambda\,V_D+a_E \quad (10)$$

$$\dot{V}_D=-\dot{\lambda}V_N-\left(\dot{\mu}+2\omega^e\right)\cos\lambda V_E+a_D \quad (11)$$

The translational kinematic equations, relating vehicle-carried NED acceleration states to body-fixed acceleration states, are given by:

$$\begin{Bmatrix}a_N\\ a_E\\ a_D\end{Bmatrix}=J_{BE}^{-1}\begin{Bmatrix}a_x^b\\ a_y^b\\ a_z^b\end{Bmatrix} \quad (12)$$

where, J^{-1}_{BE} is the inverse of the transformation matrix which rotates from the body frame to the vehicle-carried NED frame. The parameters of equations from 6-11 are defined and derived based on the World Geodetic System 84 (WGS 84) which was originally proposed in 1984 and lastly updated in 2004 (NIMA., 2000).

Forces and moments calculation: During flight there are two kinds of forces acting on Projectile motion. They are weight and resultant body and canards aerodynamic forces. The aerodynamic forces and moments are calculated within the flight simulation using the aerodynamic coefficients that predicted using PRODAS program. The total force acting on the projectile can be expressed as:

$$\begin{Bmatrix} F_X \\ F_Y \\ F_Z \end{Bmatrix} = \begin{Bmatrix} F_{WX} \\ F_{WY} \\ F_{WZ} \end{Bmatrix} + \begin{Bmatrix} F_{AX} \\ F_{AY} \\ F_{AZ} \end{Bmatrix} + \begin{Bmatrix} F_{MX} \\ F_{MY} \\ F_{MZ} \end{Bmatrix} + \begin{Bmatrix} F_{CX} \\ F_{CY} \\ F_{CZ} \end{Bmatrix} \quad (13)$$

$$\begin{Bmatrix} F_{WX} \\ F_{WY} \\ F_{WZ} \end{Bmatrix} = mg \begin{bmatrix} -\sin\theta \\ \sin\varphi\cos\theta \\ \cos\varphi\cos\theta \end{bmatrix} \quad (14)$$

$$\begin{Bmatrix} F_{AX} \\ F_{AY} \\ F_{AZ} \end{Bmatrix} = -\bar{q}S \begin{bmatrix} C_D \\ C_{N\alpha}\beta \\ C_{N\alpha}\alpha \end{bmatrix} \quad (15)$$

$$\begin{Bmatrix} F_{MX} \\ F_{MY} \\ F_{MZ} \end{Bmatrix} = \bar{q}S\left(\frac{PD}{V_t}\right) \begin{bmatrix} 0 \\ C_{Yp\alpha}\alpha \\ -C_{Yp\alpha}\beta \end{bmatrix} \quad (16)$$

where, V_t is the body velocity magnitude and given by:

$$V_t = \sqrt{u^2 + v^2 + w^2} \quad (17)$$

The lateral and longitudinal aerodynamic angles of attack, respectively, are computed as:

$$\beta = \sin^{-1}(v/V_t), \quad \alpha = \tan^{-1}(w/u) \quad (18)$$

These forces are expressed in the body-fixed frame and split into contributions due to weight (W), body aerodynamic and canard (C) aerodynamic forces, respectively. The body aerodynamic forces split into a standard aerodynamic (A) and magnus (M) forces, respectively. The total moments acting on the projectile can be expressed by:

$$\begin{Bmatrix} L \\ M \\ N \end{Bmatrix} = \begin{Bmatrix} L_A \\ M_A \\ N_A \end{Bmatrix} + \begin{Bmatrix} L_M \\ M_M \\ N_M \end{Bmatrix} + \begin{Bmatrix} L_C \\ M_C \\ N_C \end{Bmatrix} \quad (19)$$

$$\begin{Bmatrix} L_A \\ M_A \\ N_A \end{Bmatrix} = \bar{q}SD \begin{bmatrix} (PD/V_t)C_{lp} + C_{l\delta}\,\delta_F \\ (qD/V_t)C_{mq} + C_{m\alpha}\alpha \\ (rD/V_t)C_{nr} - C_{m\alpha}\beta \end{bmatrix} \quad (20)$$

$$\begin{Bmatrix} L_M \\ M_M \\ N_M \end{Bmatrix} = \bar{q}SD\left(\frac{PD}{V_t}\right) \begin{bmatrix} 0 \\ C_{np\alpha}\beta \\ C_{np\alpha}\alpha \end{bmatrix} \quad (21)$$

$$C_{m\alpha} = C_{N\alpha}((X_{CG}-X_{CP})/L_{ref} \quad (22)$$

These moments contain body aerodynamic (A), Magnus (M) and canard aerodynamic moments (C), respectively. The aerodynamic coefficients and the center of pressure location (relative to nose) are all a function of local Mach number at the mass center of the projectile. Computationally, these Mach number dependent parameters are obtained by a table lookup scheme using linear interpolation. Each canard is modeled as a point force on the projectile body, where this model was described and investigated by Elsaadany and Wen-Jun (2014). The lift L and drag D of each canard is computed by:

$$L_C = \bar{q}_C S_C C_{Lc} \alpha_C \quad (23)$$

$$D_C = \bar{q}_C S_C C_{Dc} \quad (24)$$

where, S_C is the reference area for one canard. $\bar{q}_C$ is the dynamic pressure computed using the local aerodynamic velocity at the canard computation point. C_{Lc} and C_{Dc} are the canard lift and drag aerodynamic coefficients, respectively. The canard lift and drag aerodynamic coefficients are also Mach number dependent. Computationally, they are obtained by a table look-up scheme using linear interpolation.

Atmospheric model: Variations in meteorological conditions have an effect on the projectile traveling through the atmosphere and hence affect its trajectory. The artillery projectile typically has peak altitudes of about 20 km which is within the troposphere and is thus subjected to air density and drag. With increasing altitude, air properties such as density, temperature, pressure and air viscosity change. Therefore, this changing is taken into the consideration during the trajectory calculation to get an accurate prediction. For this purpose, a standard atmosphere model is developed based on the International Standard Atmosphere (ISA) as described by Gyatt (2006). Expressions for air density, ρ and speed of sound, a, as a function of altitude, Z, can be derived and are given by:

$$\rho = \rho_0 (T/T_0)^{\left(\frac{g}{RL}-1\right)} e^{\left(g(Z_{trop}-Z)/RT\right)} \quad (25)$$

$$a = \sqrt{\gamma R T} \quad (26)$$

where, T is the air temperature and is given by:

$$T = T_0\text{-}LZ \quad (27)$$

where, ρ_0 and T_0 are the air density and air temperature at the sea level, respectively. g, R, L, Z_{trop} and γ are gravity acceleration, real gas constant for air, temperature lapse rate, tropopause altitude and adiabatic gas constant, respectively. Figure 1 depicts the variation of the air density, sound speed, air temperature and air pressure as a function of altitude.

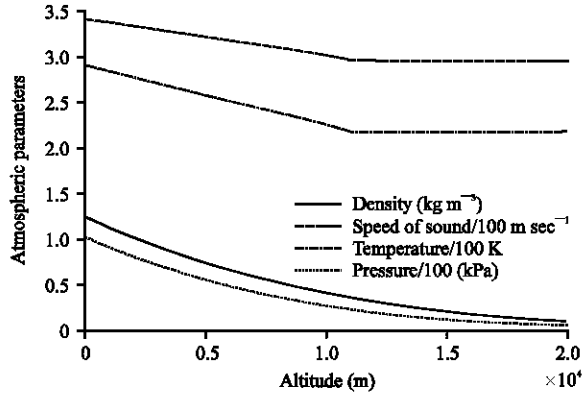

Fig. 1: Atmospheric parameters versus altitude

Simulation conditions: The developed nonlinear 6-DOF model in this study uses the physical properties of the utilized 155 mm fin-stabilized projectile in the present case study. These physical properties are listed in Table 1. Trajectory simulations have been performed in the following flight conditions: Muzzle velocity, V_0 = 810 m sec^{-1} and initial elevation angle, θ_0 = 48°.

Aerodynamic coefficients: The body non-dimensional aerodynamic coefficients and the center of pressure location that predicted using PRODAS program (Arrow Tech Associates, 2010), based on the projectile dimensions listed in Table 1, are shown in Fig. 2. The canard aerodynamic coefficients and center of pressure location are shown in Fig. 3. Note that, the presences of canard aerodynamic coefficients are considered only in the external force and moment terms in the 6-DOF equations of motion.

Table 1: Projectile physical properties

Parameters	Value
Caliber (D) (m)	0.155
Length (l) (m)	1.828
Total mass (m) (kg)	54.000
Center of gravity from nose (X_{CG}) (m)	0.838
Axial moment of inertia (I_{XX}) (kg m^2)	0.192
Lateral moment of inertia (I_{YY}, I_{ZZ}) (kg m^2)	7.563

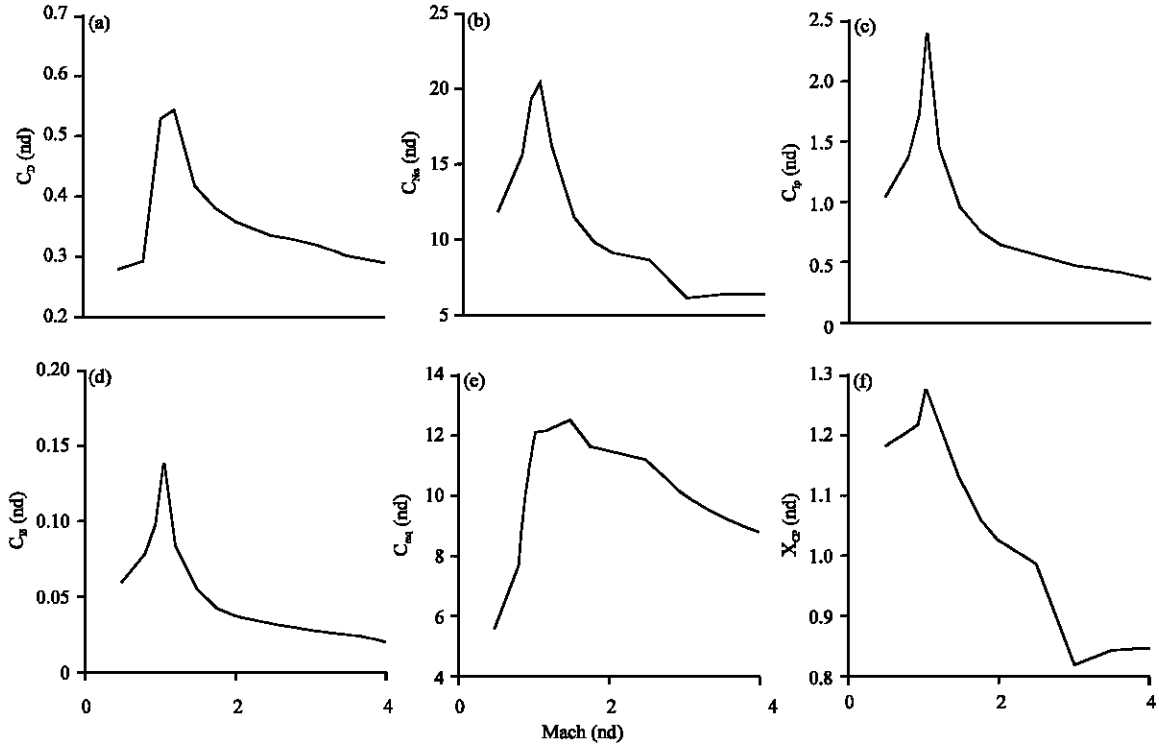

Fig. 2(a-f): Body aerodynamic parameters versus Mach number, (a) C_D, (b) $C_{N\alpha}$, (c) C_{lp}, (d) $C_{l\delta}$, (e) C_{mq} and (f) X_{CP}

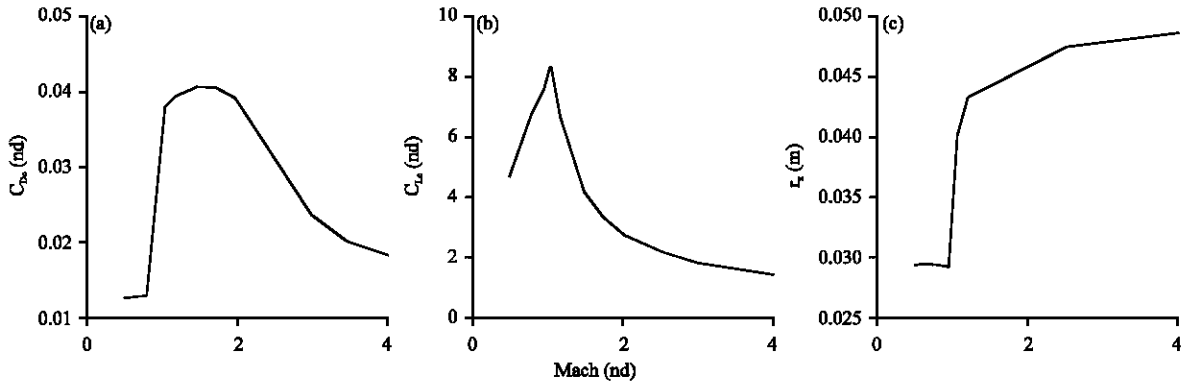

Fig. 3(a-c): Canard aerodynamic parameters, (a) C_{Dc}, (b) C_{Lc} and (c) r_x versus Mach number

RESULTS AND DISCUSSION

Range extension and performance analysis: The extended range is accomplished in this study with a four equally spaced canards, each with a reference area of 0.006525 m^2. These canards are mounted on the front of a fin stabilized projectile (our case study) provide sufficient control authority to enable extended range. At the apex of flight, the four canards are deployed and deflected by a predetermined deflection angles as a function of time. For the purpose of range extension, a proportional Plus Integral (PI) roll control system is used to get zero roll-rate and roll-angle. Since both canards in the pitch plane of the projectile that effect pitch maneuvers are deflected by angle of 8° plus the canard deflection to null roll rate, while both canards in the yaw plane are deflected by the canard deflection to null roll rate only. A nonzero canard deflection is necessary to null roll-rate, because the aft fins are canted by small angle to provide a sufficient rolling for the projectile in steady state (before the canards extension). Figure 4 and 5 demonstrate computational results contrasting the nominal and extended trajectories for the proposed projectile in the flight conditions described above. Figure 4 demonstrates that the range is extended by nearly double from 20.7-40.5 km by commanding a full authority pitch maneuver at the trajectory's maximum altitude. Previous study by Costello (1995) showed that the estimated range of a fin stabilized projectile using controllable canards can be extended by about 148%. However, the increases in the extended range due to the use of a larger size of the movable canards.

While the canard configuration can significantly increase range, it also has a large increase in overall time of flight from approximately 80-160 sec.

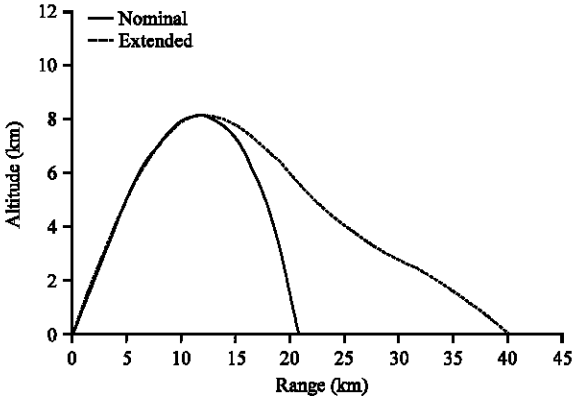

Fig. 4: Altitude versus range for nominal and extended cases

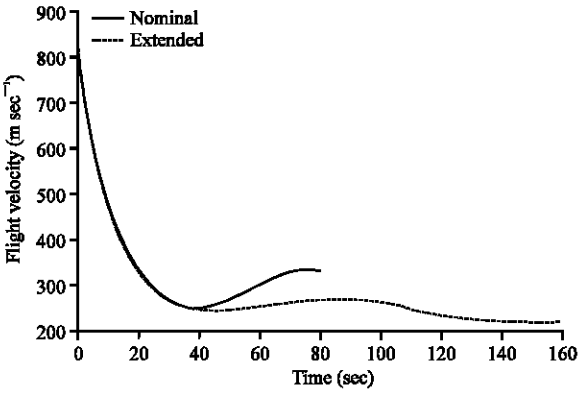

Fig. 5: Flight velocity versus time for nominal and extended cases

Figure 5 demonstrates the nominal trajectory impacts the target with a velocity of 324.7 m sec^{-1} compared to the extended trajectory with a velocity of 211.8 m sec^{-1}.

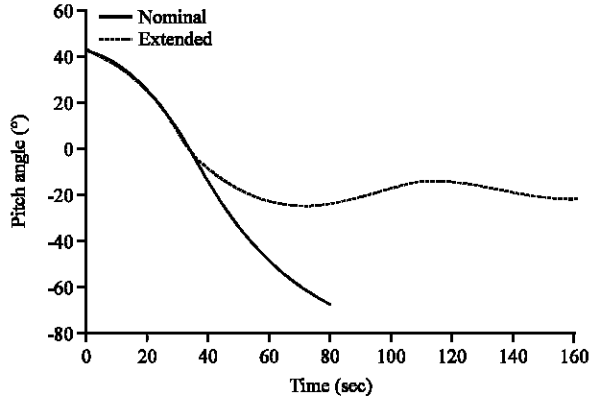

Fig. 6: Pitch angle versus time for nominal and extended cases

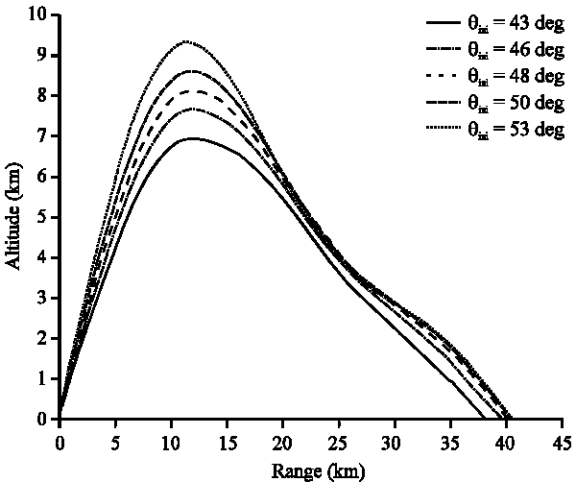

Fig. 7: Trajectories versus launch angles

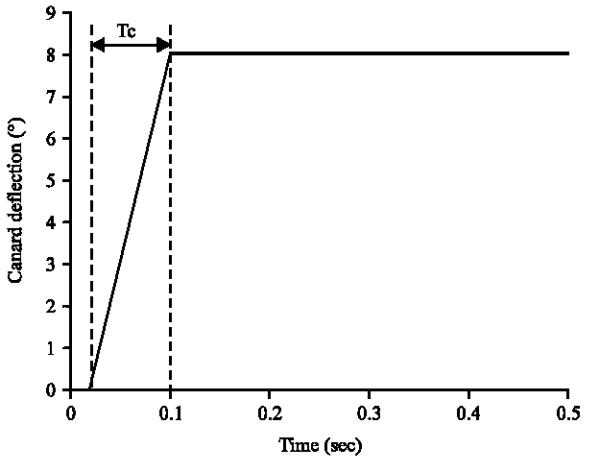

Fig. 8: Canard deflection rate (T_C)

Figure 6 demonstrates the variation of the elevation angle of the projectile versus flight time in both nominal and extended cases. The elevation angle starting from 48° at launch and decreases until reached to 0° at the summit point then in nominal case, it decreases again until reached to -64° at the impact point while in the extended case, it faces some transient oscillations. After the settlement of transient oscillations, the pitch angle approaches the value of -19° at the impact point.

Table 2: Example parameters verses launch angles

Firing angle (°)	Range (km)	Max. altitude (km)	Deployment time (sec)
43	38.094	6.945	32.78
46	39.522	7.650	34.59
48	40.132	8.123	35.72
50	40.491	8.597	36.84
53	40.477	9.304	38.52

Recall that, at the ideal trajectory (when air resistance is neglected), the maximum range is attained for a launch angle of 45°. Use the developed model (with air resistance, the upgraded density dependence on altitude, the Earth rotation and etc.), need to determine the new launch angle at which the maximum extended range occurs. Figure 7 illustrates comparative predicted extended trajectories of the proposed projectile for various launch angles. It is observed that the maximum altitude of the trajectory increases as the launch angle increases, while the maximum range occurred at launch angle of value 50°. The obtained range, maximum altitude and canard deployment time values for each launch angle are illustrated in Table 2.

Canard parametric comparison: In this section, the canard dynamic has been characterized by aerodynamic computations and 6-DOF flight dynamics investigations in order to analyze and hierarchize effects on the overall aerodynamic changing of the projectile body:

- **Canard deflection rate:** It is interesting to study the behavior of the projectile when changing the canards dynamic, i.e., the canards deflection rate as shown in Fig. 8. Hence, in this section, the influence of the canards deflection rate, T_C, is demonstrated. Figure 9 shows the effect of varying the canards deflection time, T_C, on the projectile angle of attack. It is clearly appear that the oscillation of the angle of attack is less important as the deflection rate is growing
- **Canard configuration and deflection angle variations:** Figure 10 and 11 demonstrate range and flight time for various canard configurations and various canard deflection angles. The assumption, of all canards configurations share the same aerodynamic parameters, is considered, as shown in Fig. 3. For all data points in Fig. 10 and 11, the canard

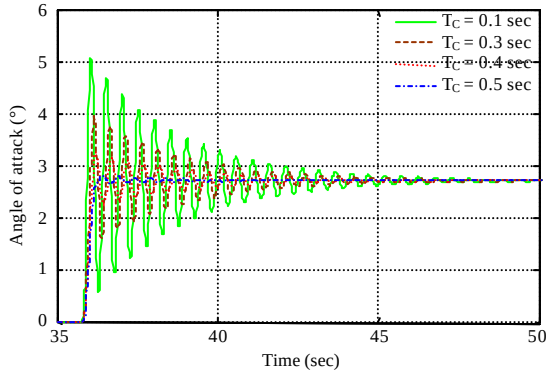

Fig. 9: Angle of attack versus time for different T_C

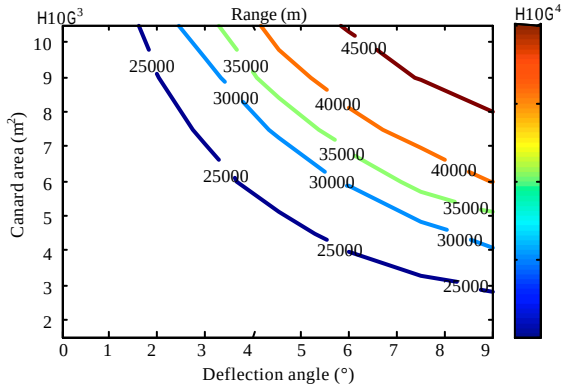

Fig. 10: Range versus canard area and canard deflection angle

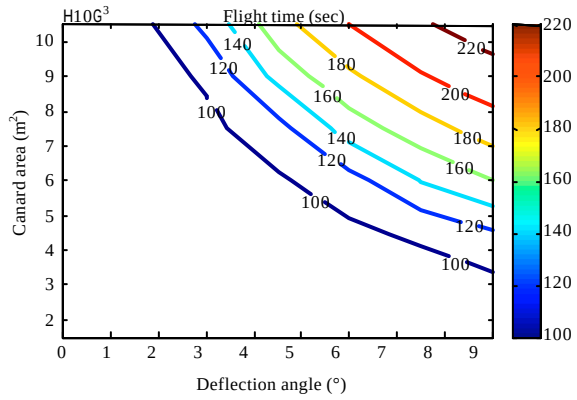

Fig. 11: Flight time versus canard area and canard deflection angle

deflection is executed at the apex of flight. As would be expected, increasing canard area or canard deflection angle increases range and thus increases the total flight time

Fig. 12: Range versus canard deployment time

- **Canard deployment time:** In this section, the analysis is carried out for deploying the canards (with no deflection) at various stages of trajectory and once the canards are deployed, it will remain open throughout the trajectory. Figure 12 demonstrates that the obtained range for various canards deployment times. The results demonstrate that the maximum range is observed when the canards are deployed at the trajectory's maximum altitude, i.e., at the apex of flight

CONCLUSION

A mathematical nonlinear model of a fin stabilized projectile equipped with a four movable canards lifting surfaces has been developed. Prediction of the response of the developed projectile model is investigated. Results clarify that the range can be extended by nearly double from 20.7- 40.5 km by commanding a full authority pitch maneuver at the trajectory's maximum altitude. It is also clarify that a significant reduction in impact velocity from approximately 324.7-211.8 m sec^{-1}. A parametric analysis varying launch angle, canard deflection angle and canard lifting surface area is achieved. It is concluded that, increasing canard area or canard deflection angle increases the extended range. Moreover, maximum extended range is obtained when the canards are deployed at the apex of flight. In addition, the influence of the canards deflection rate is demonstrated and found that the oscillation of the projectile angle of attack which occurred due to canards extension, is less important as the deflection rate is growing.

ACKNOWLEDGMENT

The research was supported by the Research Fund for the National Key Laboratory, Nanjing University of Science and Technology, China.

REFERENCES

Arrow Tech Associates, 2010. Arrow Tech software product: PRODAS V3.5. Arrow Tech Associates, USA.

Costello, M.F., 1995. Range extension and accuracy improvement of an advanced projectile using canard control. Proceedings of the AIAA Atmospheric Flight Mechanics Conference, August 7-10, 1995, American Institute of Aeronautics and Astronautics, Baltimore, MD., pp: 324-331.

Costello, M.F., 1997. Potential field artillery projectile improvement using movable canards. ARL-TR-1344, April 1997, U.S. Army Research Laboratory, Aberdeen Proving Ground, MD., USA.

Elsaadany, A. and Y. Wen-Jun, 2014. Accuracy improvement capability of advanced projectile based on course correction fuze concept. Scient. World J. 10.1155/2014/273450

Etkin, B., 2005. Dynamics of Atmospheric Flight. Dover Publications Inc., New York, ISBN-13: 978-0486445229, Pages: 592.

Gyatt, G., 2006. The standard atmosphere. http://www.atmosculator.com/The%20Standard%20Atmosphere.html

McCoy, R.L., 2012. Modern Exterior Ballistics. 2nd Edn., Schiffer, Attlen, PA., ISBN-13: 978-0764338250, Pages: 328.

NIMA., 2000. Department of defense world geodetic system 1984: Its definition and relationship with local geodetic systems. National Imagery and Mapping Agency (NIMA) Technical Report 8350.2, 3rd Edition, Amendment 1, January 3, 2000.

Ollerenshaw, D. and M. Costello, 2008. Model predictive control of a direct fire projectile equipped with canards. J. Dyn. Syst. Meas. Control, Vol. 130. 10.1115/1.2957624.

Rogers, J. and M. Costello, 2010. Design of a roll-stabilized mortar projectile with reciprocating canards. J. Guidance Control Dyn., 33: 1026-1034.